Front. Phys. China, 2010, 5(4): 357–368
DOI 10.1007/s11467-010-0108-5

MINI-REVIEW ARTICLE

Surface dynamics studied by time-dependent tunneling current

Qin LIU (刘琴), **Ke-dong WANG** (王克东), **Xu-dong XIAO** (肖旭东)†

Department of Physics, The Chinese University of Hong Kong, Shatin, New Territory, Hong Kong, China
E-mail: †xdxiao@phy.cuhk.edu.hk

Received May 31, 2010; accepted July 1, 2010

Scanning tunneling microscopy (STM) is not only an excellent tool for the study of static geometric structures and electronic structures of surfaces due to its high spatial and energy resolution, but also a powerful tool for the study of surface dynamic behaviors, including surface diffusion, molecular rotation, and surface chemical reactions. Because of the limitation of the scanning speed, the video-STM technique cannot study the fast dynamic processes. Alternatively, a time-dependent tunneling current, *I*–*t* curve, method is employed in the research of fast dynamic processes. Usually, this method can detect about 1000 times faster dynamic processes than the traditional video-STM method. When placing the STM tip over a certain interesting position on the sample surface, the changing of tunneling current induced by the surface dynamic phenomena can be recorded as a function of time. In this article, we review the applications of the time-dependent tunneling current method to the studies of surface dynamic phenomena in recent years, especially on surface diffusion, molecular rotation, molecular switching, and chemical reaction.

Keywords scanning tunneling microscopy (STM), surface dynamics, surface diffusion, molecular rotation, surface chemical reactions

PACS numbers 68.37.Ef, 68.35.Fx, 68.35.Md

Contents

1 Introduction

With the introduction and commercial availability of ultra-high vacuum systems since the 1960s [1], the probe of materials in a surface-specific fashion has become possible. Motivated by the goal of better understanding the mechanisms of heterogeneous catalysis, corrosion of materials, and fabrication of semiconductors [2], numerous new techniques were devised to investigate the structures, electronic and chemical properties of surfaces at atomic scale.

As the most outstanding technique, scanning tunneling microscopy (STM) has become a popular experimental tool since its invention [3] for the study of static geometric structures and electronic structures on surfaces due to its high spatial and energy resolution. More powerful than field emission microscopy (FEM) [4–6] and field ion microscopy (FIM) [7–9], STM is a versatile tool for direct observation of atomic-scale structures and dynamics. Various STM-based techniques [10, 11] have provided direct observations and characterizations of single molecule phenomenon, including diffusion [12], reversible switching/rotation [13], dissociation [14, 15], desorption [16, 17], and adsorption [18].

Dynamics and its control of a single atom/molecule on surfaces is an important subject in surface science. An ideal experimental technique for surface dynamics study should have both good spatial resolution and time resolution. However, the time resolution of traditional STM-based techniques, like video-STM mode, which is operated by taking images of the same area frame by frame, limits their application in the research of fast dynamic processes. Thus, it is very desirable to im-

prove the time resolution of the STM-based technique. We show here an STM-based time-dependent tunneling current, I–t curve, method that increases the capability of STM in studying fast surface dynamic processes, including surface diffusion, molecular rotation, and surface chemical reaction [12, 13, 19]. By varying the interaction strength between the STM tip and the surface adsorbed atom/molecule, the I–t curve method can be used from solely monitoring the surface dynamic processes to both monitoring and stimulating changes of surface dynamics, such as tip-induced molecular rotation/molecular switch [13] and surface chemical reaction [19].

2 Surface diffusion

Surface diffusion is an important subject in physics, chemistry, biology, and materials science. It plays a vital role in chemical and surface catalytic reaction, self-assembly, crystal growth, and thin film epitaxy [20–24]. To describe a surface diffusion phenomenon, the most important parameters are the diffusion coefficient and the diffusion activation energy. The diffusion coefficient has two different definitions: the tracer diffusion coefficient D^* and the collective diffusion coefficient D.

For a single particle executing a random walk on a surface, the tracer diffusion coefficient D^* is defined through the mean square displacement by:

$$\langle \boldsymbol{r}^2 \rangle = 4D^* t \tag{1}$$

$$D^* = \frac{1}{4} a^2 \nu_{\text{eff}} \tag{2}$$

where t is the time, a is the hopping length, and ν_{eff} is the effective hopping frequency.

According to the Arrhenius law [25], D^* can be further expressed as:

$$\begin{aligned} D^* &= \frac{1}{4} a^2 v_0 \exp\left[-E_a/(k_{\text{B}}T)\right] \\ &= D_0^* \exp\left[-E_a/(k_{\text{B}}T)\right] \end{aligned} \tag{3}$$

where the prefactor v_0 is the classical attempt frequency, E_a is the diffusion activation energy, k_{B} is the Boltzmann constant, T is the temperature, and D_0^* is the diffusion prefactor.

The collective diffusion coefficient D is defined through Fick's law [26]:

$$\frac{\partial \theta}{\partial t} = D \nabla^2 \theta \tag{4}$$

where θ is the surface coverage of the diffusing particles. Based on Arrhenius law [25],

$$D = D_0 \exp\left[-E_a/(K_{\text{B}}T)\right] \tag{5}$$

here D_0 is the diffusion prefactor.

Generally speaking, D and D^* cannot be simply related. In the case where the cross-correlations between the particle velocities are absent or can be neglected, D and D^* can be related by the following Darken equation [20, 23, 27]:

$$\frac{D}{D^*} = \left[\frac{\partial(\mu/(k_{\text{B}}T))}{\partial(\ln\theta)}\right]_T \tag{6}$$

where μ is chemical potential. In the simplest case, when the adsorbate interactions are neglected and only site exclusions are considered, the relation would be: $D = D^*/(1-\theta)$.

Experimentally, measuring any one of these diffusion coefficients may bring good understanding to the diffusion system. In the past, the observation and understanding of surface diffusion phenomenon largely depend on the development of techniques [20, 23]. Most of the diffusion measurement techniques focus on the study of the collective diffusion coefficient D. For example, the field emitter via shadowing (FE) [28], field-emission fluctuation [29], time-resolved infrared spectroscopy (IRAS) [30, 31], laser-induced thermal desorption (LITD) [32], high resolution electron energy loss spectroscopy (HREELS) [33] and linear optical diffraction (LOD) technique [34, 35–38] are some representatives.

STM is an ideal tool for tracer diffusion study although it is also reported to be able to study the collective diffusion coefficient [39, 40]. The advantage of STM is to directly provide the atomistic mechanisms of diffusion through imaging [22–24, 41–44], not only measuring the diffusion coefficient but also revealing the information about the adsorption sites and even the diffusion paths. The high spatial resolution of STM makes it possible to directly record a diffusion process at atomic scale in a frame by frame manner (video-STM mode) [10]. With the help of a lateral feedback, the STM tip is made able to follow the motion of a diffusion atom/molecule and exhibits the trace of the moving atom/molecule, resulting in an atom tracking method [11]. Unfortunately, restricted by the response of electronic feedback loops, the time resolution of these traditional STM-based techniques severely limits their application in the research of fast diffusion process. It only allows measurements of slow diffusion rates from 10^{-19} cm^2/s to 10^{-14} cm^2/s, as compared to the wide range from 10^{-19} cm^2/s to 10^{-5} cm^2/s covered by the collection of different techniques [23]. To overcome such limit, we developed a new STM-based method, I–t curve method, which fixes the STM tip position in space and records time-dependent tunneling current caused by a random walking atom/molecule between the STM tip and a given surface site. Figure 1 shows the principle of this STM mode for diffusion measurement. In this mode, the STM feedback loop is temporarily turned off while acquiring a time-dependent tunneling current curve (I–t curve) between the station-

ary STM tip and a fixed position (e.g., an adsorption site) on the sample surface. The residence of a diffusing atom/molecule on this position will cause a change in tunneling current. Thus, the time-dependent tunneling current would then be encoded with the information of the residence time of the diffusing particle at the given site [Fig. 1(b)] and provides a method to measure ν_{eff} in Eq. (2). Compared to the video-STM mode and the atom tracking mode which can only record diffusion rate as fast as ∼100 Hz [10, 11], this new mode can expand this range to $\sim 10^5$Hz using the vendor's preamplifier (cutoff frequency 100 kHz) [12]. Further improvement is possible if a customer-made fast preamplifier is available. This mode not only leads to significant overlaps in measurable diffusion rate with other techniques while retaining the atomic resolution, but also improves data statistics by acquiring a large number of diffusion events (∼200 – 500) within a reasonable time period for fast diffusion.

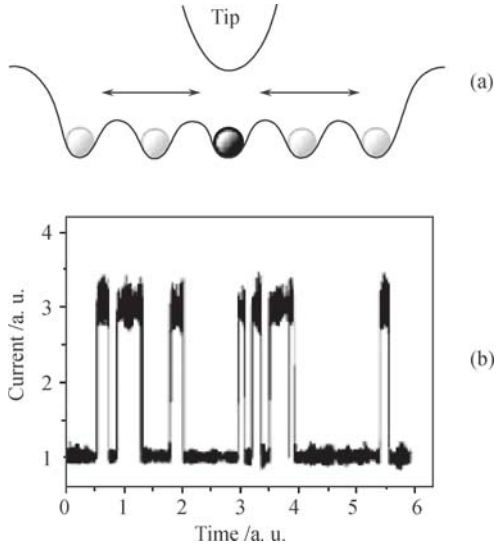

Fig. 1 **(a)** A sketch of the operational principle for diffusive hopping measurement using a stationary STM tip. **(b)** A possible I–t curve one would get when using the I–t method to study surface diffusion. Reproduced from Ref. [12].

2.1 Ag/Si(111)-7 × 7

Our group has applied this new STM-based method to study surface diffusion and demonstrated the improvement of time resolution by three orders of magnitude [12].

Because the STM tip is fixed in space during the measurement, the I–t curve method has to rely on the diffusion atom/molecule to visit the prescribed surface site. To ensure the frequency of the visit events at a given surface site, we confine a diffusing atom with a nanostructure. A natural choice of such a structure is the unit cell of Si(111)-7×7. When a Ag atom is deposited onto Si(111)-7×7 surface, it will hop inside the triangular half unit cells (HUC), as shown in Fig. 2, resulting in the Ag atom repeatedly passing through an adsorption site. In these STM images, the Si adatoms of the substrate appear bright and the faulted half unit cell (FHUC) appears brighter than the unfaulted half unit cell (UHUC) [45]. The much brighter triangular patterns, each with six bright spots, three at the corners and three at the centers as indicated in Fig. 2(a) at room temperature are known to originate from a single Ag atom hopping frequently from site to site within the half unit cell. In fact, the diffusion activation energies for an Ag atom to hop out of the UHUC and FHUC are 810 meV and 930 meV, respectively [46]. These values are much larger than the diffusion activation energies for an Ag atom to diffuse inside any HUCs, which is lower than 300 meV as will be seen later [47]. Therefore, at not so high temperatures, the Ag atom is trapped inside HUCs. As shown in Fig. 2(b), when the sample was cooled down to 78 K, single bright spots at the corner Si adatom sites were imaged for a single Ag atom in the FHUC. At 5 K [Fig. 2(c)], the Ag atom in the UHUC also ceased hopping and the bright spot at the center Si adatom site was imaged. These images provide the information of stable Ag adsorption sites on Si(111)-7×7 surface. In fact, each bright spot here is correlated with, but does not necessarily represent, the Ag adsorption site [48]. As uncovered by the density functional calculations, the single Ag atom actually prefers high coordination sites on Si(111)-7×7 surface [S and S' sites in Fig. 3(b)], instead of the top site of Si adatoms [47–49]. In FHUC, the stable adsorption site is the S site, while in UHUC, it

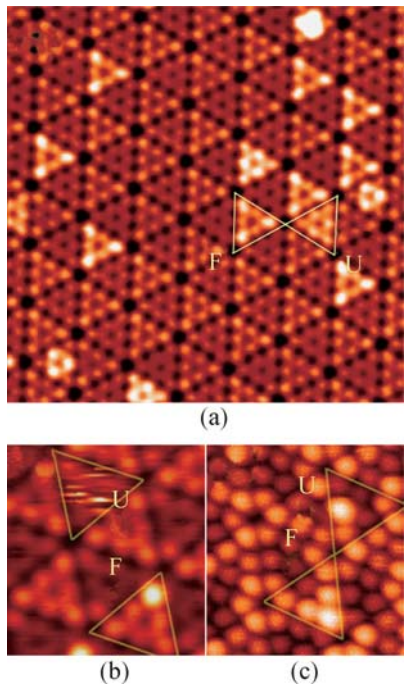

Fig. 2 Topographic STM images of Ag on Si(111)-7×7 at **(a)** 298, **(b)** 78, and **(c)** 5 K. The tunneling current and sample bias are set at 50 pA and –2 V, respectively. The fuzzy image in UHUC at 78 K is due to the nonfrozen motion of Ag. Reproduced from Ref. [48].

is the S' site. The apparent different positions between the bright STM image spot and the stable adsorption site was found to be caused by electronic effect [48]. According to the dimer-adatom-stacking fault (DAS) model [50] [Fig. 3(a)], the atomic structures of the top Si surface layers in the two HUCs are basically mirrored with respect to the line through the Si dimer rows. Because the stacking fault is between the third and fourth Si layers from the surface, its effect on the adsorbates is usually negligible except an overall lowering of potential energy in FHUC [51–54], thus a strong asymmetry is not expected. However, the different stable adsorption sites in both HUC already show an observable asymmetry in this system. An additional asymmetry in hopping dynamics is also shown in Fig. 2(b). At 78 K, single Ag atoms ceased hopping in FHUC, while they are still moving rapidly in UHUC. Since the adsorption sites can been identified through the STM images and theoretical calculations [48], we now try to use the STM-based I–t curve method to measure the tracer diffusion coefficient of Ag inside FHUC and UHUC through the effective hopping frequency ν_{eff}.

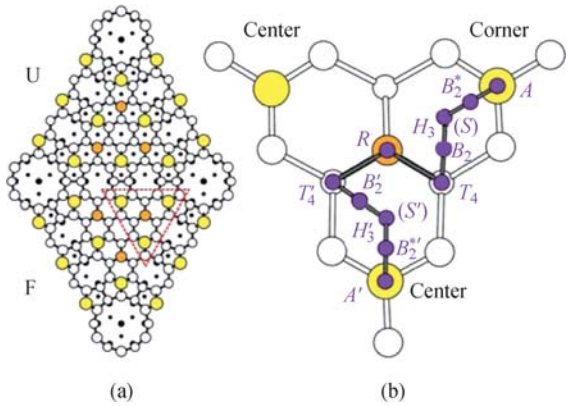

Fig. 3 The DAS model **(a)** and the basin **(b)** on which possible Ag adsorption sites are labeled. Reproduced from Refs. [48, 50].

As depicted in Fig. 4(a), we placed the STM tip over 4 different sites, the corner and center sites of both HUCs, on Ag/Si(111)-7 × 7 surface to record the I–t curve at various temperatures [47]. Figure 4(b) shows a typical two-state tunneling current signal for the STM tip positioned stationary over a corner Si-adatom site in FHUC at 144 K. The high current (∼250 pA) corresponds to an Ag atom residing at a site associated with the bright spot at the corner Si-adatom, while the low current (∼50 pA) corresponds to the Ag atom away from this site. When we place the tip over a center site in FHUC [site d in Fig. 4(a)], however, only a straight line was observed [Fig. 4(d)], indicating that the residence time of Ag atom at this site is either too short to be detected, or it never stays there. In UHUC, the dynamic behavior is completely different. As shown in Fig. 4(c) with the tip positioned over a corner Si-adatom site, one observes very "noisy" high current states that oscillates between the current baseline and the current maximum, although the low current state is similar to that in Fig. 4(a). When the tip is positioned over a center Si adatom in UHUC, a similar dual-time scale behavior is also observed Fig. 4(d). The "noise" in fact consists of spectra similar to those of Fig. 4(b) but on a much shorter time scale. These results clearly demonstrate the asymmetry of dynamics of Ag inside two HUCs.

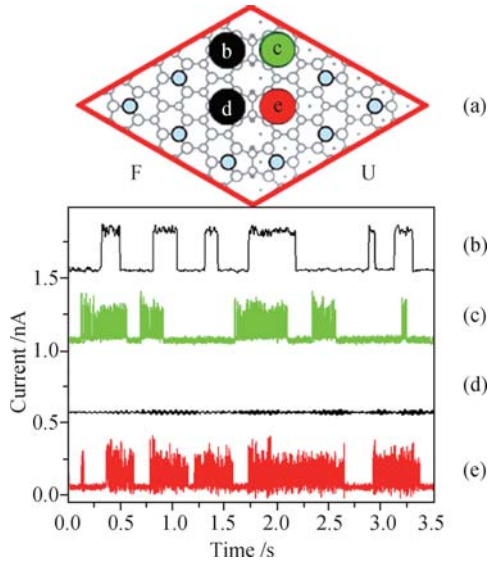

Fig. 4 **(a)** Schematics for the STM tip positions to acquire the spectra in (b) to (e). **(b)** and **(d)** Typical time-dependent tunneling spectra taken at 144 K for an STM tip above the corner and center Si-adatom in a FHUC containing a moving Ag atom. Set point –2 V, 0.05 nA. **(c)** and **(e)** Typical time-dependent tunneling spectra at 106 K for an STM tip above the corresponding sites in a UHUC with a moving Ag atom. Set point –2 V, 0.05 nA. Reproduced from Ref. [47].

To understand what causes the different dynamic behavior for Ag atoms in UHUC and FHUC, we calculated the static potential energy surface (PES) for Ag on Si(111)-7×7 by first principles method based on the density functional theory (DFT) [55, 56]. As seen in Fig. 5, the local energy minimum sites are S or S' sites instead of the Si-adatom sites, in spite of the bright spot being observed in STM images at negative bias [48]. Inside the Si(111)-7×7 half unit cells, a "basin" is defined by a triangle with the rest Si atom at the center and three surrounding Si adatoms at the corners, as shown in Fig. 3(b) [57, 58]. Therefore, there are three potential energy wells inside a basin in which the Ag atom may reside. From the PES, one can calculate that the energy barrier between S and S' site in UHUC is about 230 meV while the barrier between basins is about 340 meV. Because of the relatively low energy barrier between the sites inside a basin, the Ag atom may diffuse frequently among the three sites at elevated temperatures. Diffusion among different basins is also possible, but at a lower rate because of the higher energy barrier. In this picture, there are naturally two

time scales for the Ag atom in UHUC: diffusion within a basin and diffusion among three basins when the tip is placed above a corner Si-adatom [position c in Fig. 4(a)]; only one basin is detected. However, when the tip is placed above a center Si-adatom [position e in Fig. 4(a)], two neighboring basins are detected. This explains why there is about 30% of the time in Fig. 4(c) with noisy high current, and about 70% of the time in Fig. 4(e) with noisy high current.

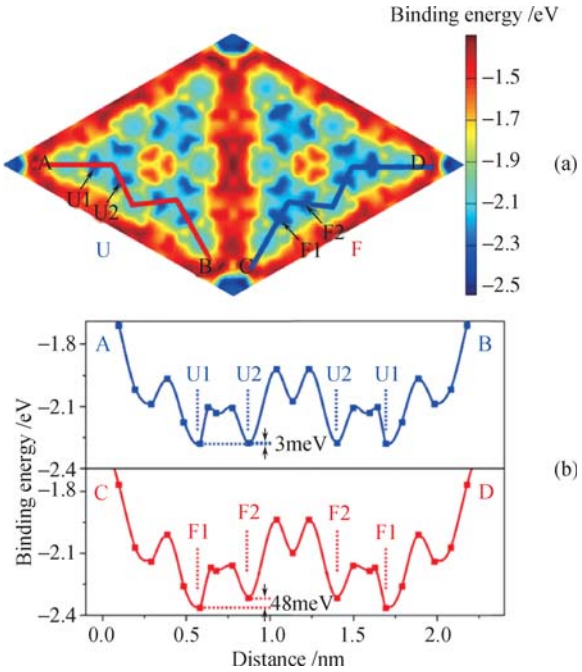

Fig. 5 **(a)** A potential energy surface for a Ag atom on Si(111)-7×7 constructed by first principles calculations. The thick lines are probable diffusion paths for Ag atom in the two half unit cells. **(b)** Potential energy along the paths outlined in (a) for both FUHC and UHUC. Reproduced from Ref. [47].

In principle, a similar dual-time scale behavior should also be observed for Ag diffusion in FHUC. In FHUC, there are also relatively high energy barriers (∼400 meV) that trap the Ag atom within one basin. However, within a given basin the adsorption energies at the corresponding F1 and F2 sites have a large difference, apparently caused by the stacking fault underneath. Experimentally, this energy difference is estimated to be larger than 80 meV, while the theoretical calculation gives a difference of 48 meV [Fig. 5(b)]. In contrast, the adsorption energies at U1 and U2 sites in UHUC differs only by < 5 meV as determined from both experiment and theory. The large difference in adsorption energy could render the residence time of Ag atom at F2 sites too short to be detected. Effectively, the Ag atom appears to reside only at F1 before hopping out to another basin. Thus, in analyzing the time-dependent tunneling spectra, for Ag in UHUC we have two hopping processes: one for intrabasin diffusion and the other for interbasin diffusion; but for Ag in FHUC, we only need to consider interbasin diffusion.

We can obtain the average residence time τ and the hopping rate $\Gamma = 1/\tau$ for an Ag atom at different sites from the statistics of the distribution of residence time recorded by the I–t curves [12]. In Fig. 6, we depict the hopping rate over 5 orders of magnitude for a number of temperatures in an Arrhenius plot for interbasin diffusion both in the FHUC and UHUC. By fitting the data, we found that the interbasin diffusion in FHUC and UHUC have comparable activation energy of $E_a =$ 270 meV and 240 meV, respectively. The measured interbasin hopping rates differ by $\sim 10^3$ times in the two half unit cells for the overlapping temperatures. The intrabasin fast diffusion in UHUC has an $E_a = 120$ meV, a value much smaller than that between two basins. The first principles calculations are in good agreement in the overall trend, but all the energy barrier values are somewhat higher than the measured ones. The accuracy of the DFT method, the non-inclusion of finite temperature entropic and dynamic effects by the DFT calculation may contribute to the over-estimations of activation energies.

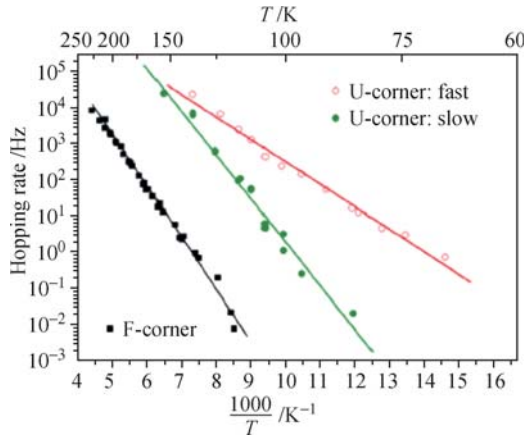

Fig. 6 Arrhenius plots of the hopping rate for Ag atoms in FHUC and UHUC. The data obtained at different bias (–0.5 V to –2.5 V) in FUHC show no bias dependence. The data shown for UHUC are obtained for STM positioned above a corner Si adatom at a bias of –0.5 V to minimize electric field effect. Reproduced from Ref. [47].

In this example, we have demonstrated that the I–t curve method can measure fast surface diffusion of particles confined in nanostructures. Using the same method, quantitative site-specific hopping rates as well as the residence time at different sites for Cu [12] and Au atoms confined in a Si(111)-7×7 half unit cell have also been unambiguously measured.

2.2 CO/Pt(111)

The key for the success of the I–t curve method in the above example is the surface potential energy heterogeneity that forces the diffusing particle to repeatedly return to the site of interest [12, 47]. It turns out that confinement potential can be lifted if there are many diffusing atoms/molecules on the surface and the waiting

time for observing hopping events is not an issue. Here, using this method we show our results of CO diffusion on the terrace of Pt(111) surface [59], where no such energy barrier that limits the motion of CO molecule exists.

Surface diffusion of CO on platinum is important for investigating the mechanisms of CO hydrogenation in the synthetic fuel industry, and CO oxidation in the automotive industry, where Pt is used as a catalyst. Detailed collective diffusion measurements of CO molecules on stepped Pt(111) surfaces have shown that CO diffusion perpendicular to surface steps is impeded because of the additional trapping at step sites [37], while diffusion parallel to steps is faster than that on terraces [36]. A possible explanation for the latter effect is that steps provide a fast diffusion channel for CO molecules to diffuse parallel to Pt steps [36]. Using the I–t curve method, we are now able to check whether this proposal is correct.

Figure 7 shows STM images of the clean Pt(111) surface and the same area after dosing 0.1 Langmuir CO. The STM image exhibits fuzzy features both on terraces and steps as indicated by the arrows in Fig. 7(b) after CO dosing. The fuzzy features are attributed to the fast hopping of CO molecules. By placing the STM tip over a terrace site or a step site, I–t curves can be recorded. It was found that on the steps, CO is adsorbed at the upper step edge [60, 61] rather than the lower step edge by previous experiments with a trapping potential of $\sim$ 300 meV larger than that on terraces [31, 37, 62–64]. Thus, the STM tip was placed over the upper step edge [Fig. 8(a)] when taking I–t curves on steps. To avoid step influence, the terrace site is chosen at least 10 nm away from the steps. Figures 8(b) and (c) show typical I–t curves taken at 141 K above such a step site and a terrace site, respectively. Since there are no lateral confinements for CO diffusion on the Pt(111) surface, the observed hopping events were significantly fewer as compared to Ag atom trapped within HUCs of Si(111)-7×7. Here, the molecule leaving the measured adsorption site may not return to the same position and it is necessary to rely on other CO molecules coming to visit the measured site. The waiting time must therefore be sufficiently long to take account of the foreseeable delay, especially on terraces. As a result, the fractional occupation time with a CO molecule on the measured site is quite small as can be seen in the I–t curves both on terraces and on steps [Fig. 8(b) and (c)].

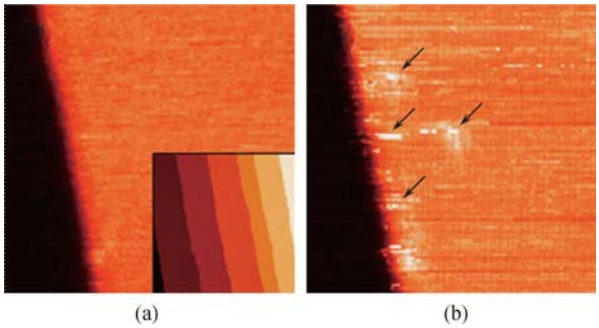

Fig. 7 **(a)** An STM image of clean Pt(111) surface (30 nm × 30 nm). *Inset*: a 250 nm × 250 nm STM image show the distribution of steps on the clean Pt(111) surface. **(b)** After a small amount of CO dosing, the Pt(111) surface becomes "noisy". Some of the bright spikes caused by the presence of CO molecules are pointed out by the arrows. Reproduced from Ref. [59].

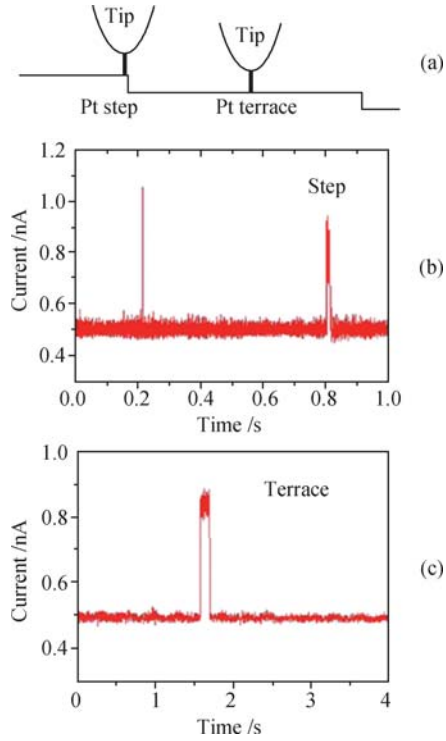

Fig. 8 **(a)** A sketch illustrating the tip positions when taking time-dependent tunneling current curves on Pt(111) steps or terraces. **(b)** and **(c)** examples of I–t curves taken on Pt(111) step and terrace, respectively. A high current region represents the presence of a CO molecule underneath the STM tip. Reproduced from Ref. [59].

The hopping rates of CO molecules along steps and on terraces at various temperatures from 103 K to 190 K were measured using the I–t curve method. The results are depicted in an Arrhenius plot in Fig. 9. The corresponding diffusion coefficients are also labeled in Fig. 9 by assuming that all the hopping events happened between two adjacent top adsorption sites. By fitting the data, we obtained the activation energy E_a on terraces and on steps to be 220 meV and 165 meV, respectively. With a trapping potential that confines the motion of CO molecules along steps, the measured value of 165 meV is the diffusion activation energy of CO molecules along steps. It is apparently lower than that on terraces. In Fig. 9, one can also find that the hopping rate of CO along steps is about 10 times faster than on terraces in the measured temperature range. Therefore, our results here provide direct evidences that the steps on Pt(111) surface act as a fast diffusion channel for CO molecules parallel to Pt(111) steps [59]. The success of measuring CO diffusion on Pt(111) also demonstrated applicability of the I–t curve

method on surface diffusion without nanometer scale lateral potential confinement.

The I–t curve method has been applied to study the diffusive motion of oxygen vacancy pairs (OVPs) on rutile TiO_2(110)-1 × 1 surface by Cui *et al.* [65]. They found that the oxygen vacancies (OVs) can be moved along the bridging oxygen rows on TiO_2(110)-1×1 by an STM tip with a bias voltage of 3.0 V. Two OVs can combine to form an oxygen vacancy pair. The hopping of OVPs at room temperature is relatively fast and cannot be recorded by the frame by frame imaging, but can be studied by the I–t curve method as shown in Fig. 10.

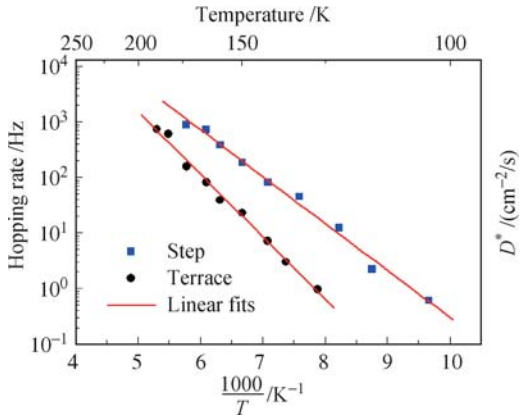

Fig. 9 Arrhenius plot of the hopping rate for CO on Pt(111) steps and terraces from 103 K to 190 K. The squares represent data for the steps, the circles data for the terraces. All the data were taken at –0.5-V bias. Reproduced from Ref. [59].

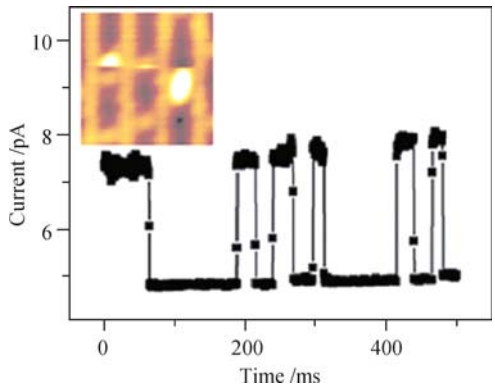

Fig. 10 A typical I–t curve taken over a diffusive OVP (see the inset: 2.5 nm × 2.5 nm) with a set point condition of 0.4 V and 5 pA at RT. Reproduced from Ref. [65].

3 Molecular rotation

Because of its capability to detect high frequency motion, the I–t curve method has become a popular technique in the study of many other molecular dynamic processes on surface, including molecular rotations, molecular switches, and surface chemical reactions. For example, the I–t curve method could be applied to measure the rotation speed of a molecular rotor formed by a single $(t-\mathrm{Bu})_4$-ZnPc molecule adsorbed on Au(111) surface [66, 67]. The so-called molecular rotor with a fixed off-center rotation axis has been observed by STM at liquid nitrogen temperature as shown in Fig. 11(a). Experiments and first-principles calculations reveal that the gold adatom on the Au(111) surface acts as a stable contact for the $(t-\mathrm{Bu})_4$-ZnPc molecule. The chemical bond between the gold adatom on the surface and the nitrogen atom in the molecule forms a hinge and acts as an off-center rotation axis. The $(t-\mathrm{Bu})_4$-ZnPc molecule can then move among various rotation-favorable configurations [Fig. 11(a)]. Figure 11(b) shows an I–t curve taken at a fixed point on the folding fan [see Fig. 11(a)] at a constant bias voltage of –1.8 V. The amplitude of the tunneling current oscillates with a high frequency between 0 and 5 nA. The oscillation indicates that the folding-fan feature is caused by molecular rotation with respect to the substrate surface. By combining the I–t curve and DFT calculations, it has been demonstrated that the configurations and corresponding adsorption energies of such a large molecular complex in a dynamical process can be identified [67].

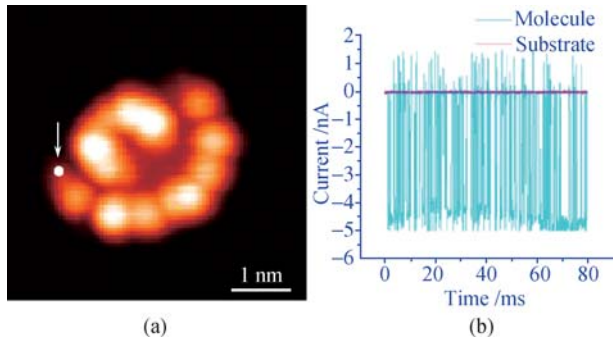

Fig. 11 **(a)** STM image of single $(t-\mathrm{Bu})_4$-ZnPc molecular rotor located at the elbow position on Au(111) surface, showing a folding fan feature. **(b)** I–t curve measured on the molecular rotor. The arrow and spot in (a) indicate the position where the I–t curve was measured. Reproduced from Ref. [66].

4 Stimulated molecular motion and chemical reactions

In all the works described above, the I–t curve method was used to study the intrinsic surface dynamics of atom/molecule caused by thermal excitations. In order not to disturb the surface dynamic process, one must work under a condition with relative weak interaction between the STM tip and surface, to reduce any possible influence of the tunneling current, the bias voltage, or the tip surface potential on the intrinsic motion of atom/molecule. As an example, when using the I–t curve method to study the hopping of a single Ag atom inside the FHUC of Si(111)-7×7 surface, the tip effect was checked as shown in Fig. 12. At 144 K, by fixing the bias voltage at –2 V, one observes that the tunneling current can greatly affect the hopping rate when the

base tunneling current is larger than 100 pA [Fig. 12(a)]. To detect the intrinsic Ag diffusion dynamics, we must work with a base tunneling current lower than 100 pA. On the other hand, by fixing the base tunneling current at 50 pA, the measured hopping rates remain basically unchanged even when the bias voltage changes from –0.7 V to –3 V [Fig. 12(b)]. So we conclude that if the set-point is set at –2 V and 50 pA, the tip effect is minor. From the two-state current signals shown in Fig. 4(b), we obtain the ratio of the total residence time of one single Ag atom on one corner FHUC site over the total measurement time to be ∼33%, consistent with a picture that the Ag atom diffuses with equal probability to three stable corner adsorption sites and verifying a negligible role of the tip when the set-point is at –2 V and 50 pA.

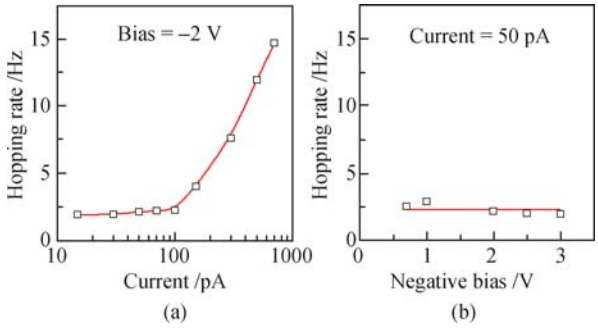

Fig. 12 Check the tip effect when using I–t method to study the Ag atom hopping in Si(111)7×7 FHUC at 144 K. **(a)** The sample bias was fixed to –2 V, the tunneling current was changed from 15 pA to 700 pA. **(b)** The tunneling current was fixed to 50 pA, the sample bias was changed from –0.7 V to –3 V.

I–t curve method can be used not only to detect motions of atoms/molecules, but also to stimulate their motions via the tip effect. As an example, inelastic electrons from the STM tunneling current can be used to induce reversible rotation of individual acetylene molecule between two diagonal sites on Cu(100) surface at low temperature [13] and the induced motions of the acetylene molecule can be monitored by the I–t curve method. The C–C bond of acetylene is parallel to Cu(100) surface and the two C atoms have a π bonding to Cu atoms as depicted in the side view of Fig. 13(a). There are two equivalent orientations for the adsorbed acetylene molecule on Cu(100) as shown in Fig. 13(a) together with their corresponding STM images. When the STM tip is positioned above the acetylene molecule, the tunneling current would undergo a fast change once the sample bias voltage is higher than the C–H stretch mode energy. Figure 13(b) shows the I–t curve with a bi-stable current level during a 364 mV voltage pulse over an acetylene molecule. The low (high) value corresponds to the orientation with the tip outside (inside) the plane of acetylene [Fig. 13(a)]. Hence, the jump in current represents the rotation of the molecule between two equivalent orientations on Cu(100) surface. The distribution of events in each current state follows an exponential decay. The inverse of the time constant of the exponential distribution gives the rotation rate of acetylene molecule for the chosen sample bias voltage and current. Figure 13(c) shows the distribution of the events in high current state and is fitted with a time constant of 184 ms, corresponding to a rotation rate about 5 Hz. The rotation rate induced per elastic electron from the tip depends on the tunneling current linearly below 10 nA. Further research demonstrates that the probability of rotation per C–H stretch excitation is tip independent and the coupling of the stretch vibration of C–H to the hindered rotational mode is the dominant reason for the observed rotation of acetylene molecule on Cu (100) surface.

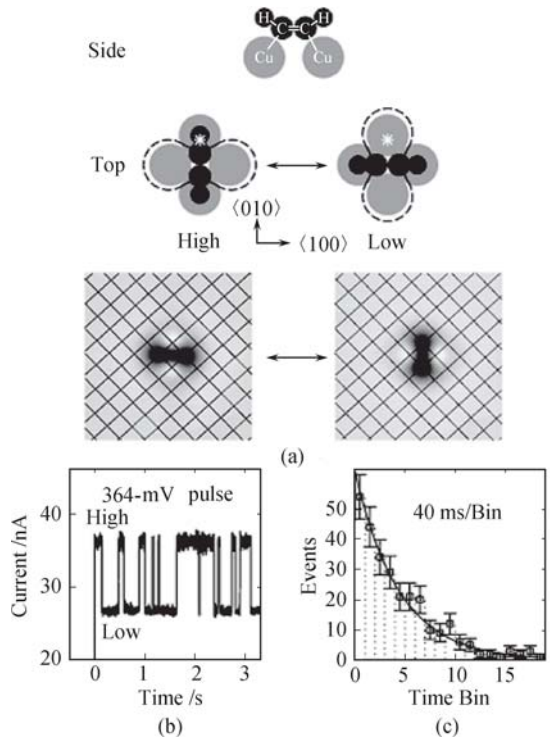

Fig. 13 **(a)** Model of the molecular adsorption site and two orientations on the surface along with corresponding STM images. **(b)** I–t curve during a 364-mV voltage pulse over a molecule. The tip is fixed 1.5 above the molecule. **(c)** Distributions of events for high current orientation. Reproduced from Ref. [13].

The above example showed a certain degree of controllability to switch between two adsorption sites. Controlled switching of a molecule between its two different stable configurations on surface may be explored as a model device of molecular switching. As the simplest basic electronic element in molecular electronics, molecular switching has become the focus of study in recent years. Molecular or suprameolecular switching consisting of single or few molecules (supramolecules) must satisfy two basic requirements [68]. First, it must have at least two different stable configurations. Then, it must be able to repeatedly inter-convert between the two configurations by external signals rather than spontaneous excitation. One important type of a molecular switching device depends on the conformation change of molecules.

Various external stimuli, such as temperature, light, or electric fields have been explored to induce conformational changes. In particular, the tunneling current or tunneling electrons injected from an STM tip can be used as an external stimulus to induce the switch of molecular states. Compared to other external stimuli, STM can provide single molecule selectivity in real space. The variations of the tunneling current in I–t curve together with STM images can display the electronically excited reversible switches. In the system of $CoCu_n$ linear molecules constructed on Cu(111) surface [69], the inelastic tunneling electron inject energy into the Co–Cu bonds and cause the Co atom to switch between two nearby adsorption sites, face-centered cubic site [fcc site shown in Fig. 14(a)] and hexagonal close-packed site [hcp site shown in Fig. 14(b)]. The I–t curve obtained in the left vicinity of Co atom in $CoCu_2$ molecule exhibits a telegraph characteristic signal [the inset of Fig. 14(c)], demonstrating the controlled switching. The distributions of residence time of Co atom in different current states also follow exponential decay as shown in previous examples.

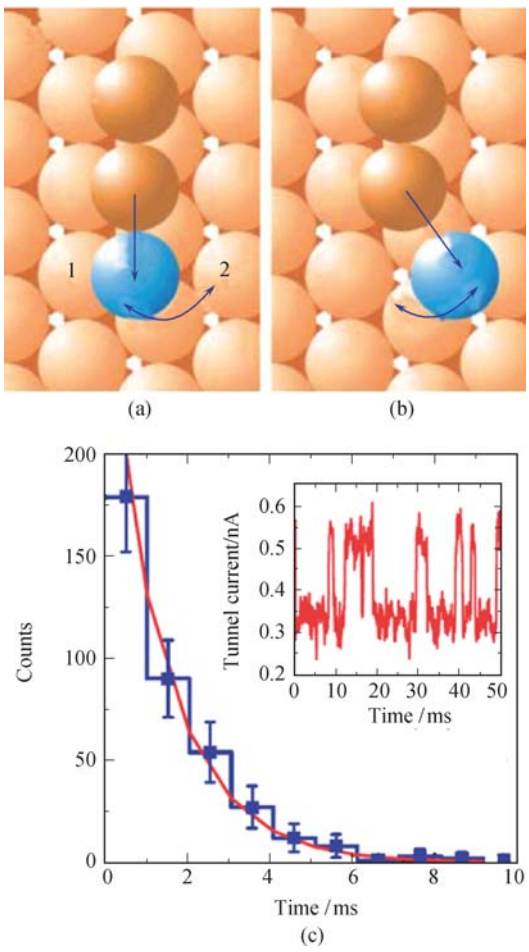

Fig. 14 Model of a $CoCu_2$ molecule on the Cu(111) substrate in **(a)** a linear and **(b)** a canted configuration, corresponding to the Co atom (*blue*) in the fcc and the hcp sites, respectively. **(c)** Distribution of residence times of the Co atom in the high current state with a fit to an exponential decay (*red line*). (Inset) A portion of the I–t curve obtained in the left vicinity of the Co atom in the $CoCu_2$ molecule at 15.4 mV sample bias. Reproduced from Ref. [69].

The switch of 4,4-azopyridine trimers in an ordered array on Au(111) is another example of a molecular switch [70, 71]. As shown in Fig. 15(a) and (b), the 4,4-azopyridine trimer can be switched between a linear shape and a bend shape via electron attachment. Three 4,4-azopyridine molecules form an ordered array of trimer, which is located at elbow sites of the Au(111)-23 $\times\sqrt{3}$ surface [72] [Fig. 15(a)]. This trimer can be reversibly switched between a linear and bent shape [Fig. 15(a) and (b)]. When the STM tip was positioned above the encircled molecule in the trimer [see Fig. 15(a)] and the sample bias V was increased to 1.5 V, the current I would undergo a steep drop. Subsequent imaging revealed that the marked molecule rotated by $\sim 30^\circ$ whereas the other two molecules remained unaltered. By repeating the procedure the rotated molecule can be switched back to its original position and a linear trimer is recovered. This process can be recorded in the I–t curves as shown in Fig. 15(c). During the switching process, single weak C–H $\cdots$ N hydrogen bonds are broken and reformed. Both the linear and bent trimers are robust and can be switched many times.

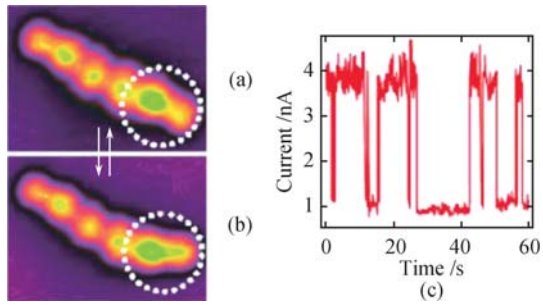

Fig. 15 **(a)** and **(b)** Reversible switching between linear and tilted 4,4-azopyridine trimer array on Au(111) induced by a 1.5-V pulse onto the marked molecule (0.2 V, 0.1 nA; 3.5 nm × 2.6 nm). **(c)** I–t curve measured on the marked molecule (a) with open feedback loop (tunneling gap parameters: 1.4 V, 4 nA). Reproduced from Ref. [70].

In the above examples of molecular switches, the interaction between the tunneling current and the molecules is strong enough to activate the switching but weak enough to retain the molecular bonding. When a much stronger interaction is employed between the STM tip and a molecule, surface chemical reactions may be induced. Again, the I–t curve can be applied to record the moment when the tip induced reaction happens and provides the details of the reaction process.

For CoPc molecule adsorbed on Au(111) surface, Zhao *et al.* [19] applied a positive sample high-voltage (more than 3.3 V) pulse over the edge of a lobe of the CoPc molecules [Fig. 16(a)], the I–t curve [Fig. 16(b)] shows two sudden drops within half a second. The change in the tunneling current is resulted from the dehydrogenation process of the CoPc molecule [73]. The two drops

in I–t curve indicate the sequential dissociation of the two H atoms from the benzene ring. Topographic image shows that the bright lobe disappeared after the voltage pulse [Fig. 16(b) *inset*]. When all four lobes were cut to obtain the final dehydrogenated CoPc (d-CoPc) molecule [Fig. 16(d)], a marked increase of ∼0.8 Å in apparent height at the center indicated either a strong conformational change of the molecular structure or a redistribution of the LDOS of the molecule. dI/dV spectra near the Fermi level measured at the center of a d-CoPc molecule show a Kondo resonance peak arises immediately below E_F. The Kondo temperature T_K of d-CoPc is further estimated to be ∼208 K. First-principles studies found that the interaction between the planar CoPc molecule and the Au substrate completely quenched the magnetic dipole moment of the Co atom. However, dehydrogenation induces a marked change of the molecular structure, so that the d-CoPc molecule on Au(111) is no longer planar. The central Co atom in the d-CoPc molecule shifts upward remarkably and the magnetic moment is recovered, leading to the Kondo effect. In this example, the detailed dehydrogenation processes were recorded by the I–t curve, which helps the identification of the mechanism of the generation of the d-CoPc molecule and hence the strong Kondo effect.

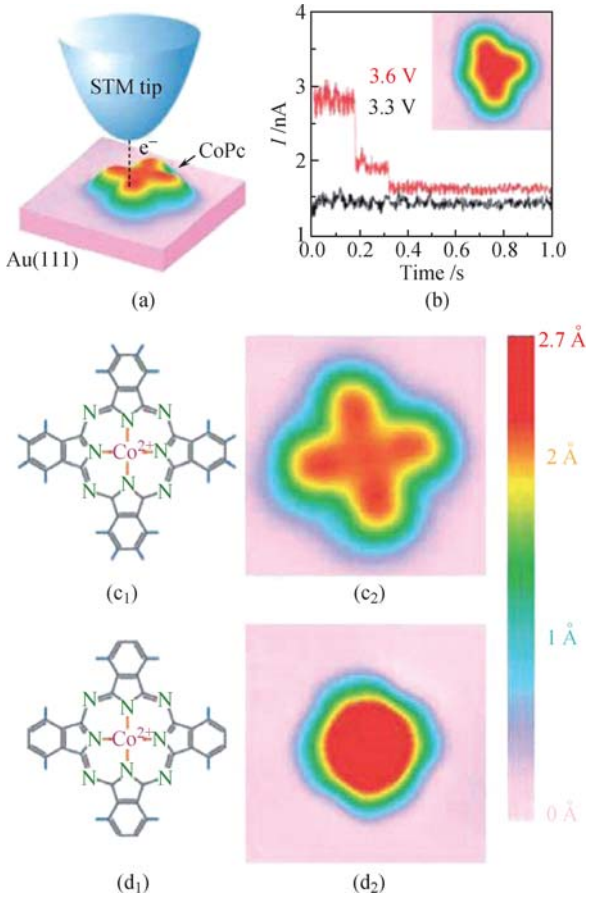

Fig. 16 STM tip-induced dehydrogenation of a single CoPc molecule. **(a)** Diagram of the dehydrogenation induced by the STM current. **(b)** I–t curve taken during two different voltage pulses applied on the brink of one lobe. Black and red lines correspond to 3.3 and 3.6 V, respectively. (b) Inset shows the result after the dehydrogenation process by one 3.6-V pulse. (**c**$_1$) and (**d**$_1$) Structural formula of a single CoPc molecule before and after four dehydrogenation processes. (**c**$_2$) and (**d**$_2$) STM images of an intact CoPc and a d-CoPc, respectively (25 Å × 25 Å). The color scale represents apparent heights, ranging from 0 (low) to 2.7 Å (high). Reproduced from Ref. [19].

5 Summary

In this review, we have used a number of examples to demonstrate that the STM-based I–t curve method has been applied to study surface dynamic behaviors, including surface diffusion, molecular rotation, molecular switching, and surface chemical reactions. Depending on the strength of interaction between the STM tip and the atom/molecule adsorbed on the surface, the I–t curve method may function just as a tool for monitoring the intrinsic motion, or function as a tool for applying a stimulus to change the states of atom/molecule. In the experiments of Ag, Cu diffusion on Si(111)-7×7 surface and the molecular rotations, this method has demonstrated its capability of detecting fast dynamic processes about three orders of magnitude higher than the traditional video-STM method. In the molecular switch experiments, the tunneling electrons with high enough energy can excite the motion of molecule under study and change its configuration reversibly. When the interaction between the tunneling electrons and the adsorbed molecule is further increased, permanent change of molecule, namely, chemical reaction was shown to be possible. In all the cases above, the change of the atom/molecule state in the adsorption site, configuration, or chemical specie can be clearly shown in the I–t curves.

Acknowledgements The works done by our group described in this paper were supported by the Direct Grant for Research from the Chinese University of Hong Kong, and the Research Grants Council of Hong Kong (RGC 604504, HKUST6152/01P, N-CUHK616/06, RGC 603803, RGC 603806, and RGC 404008).

References

1. R. W. Roberts and L. E. St. Pierre, Science, 1965, 147: 1529
2. K. W. Kolasinski, Surface Science: Foundations of Catalysis and Nanoscience, New York: Wiley, 2008
3. G. Binnig and H. Rohrer, Helv. Phys. Acta, 1982, 55: 726
4. I. Brodie, Surf. Sci., 1978, 70: 186
5. H. Heinzelmann, F. Watanabe, and G. M. McClelland, Phys. Rev. Lett., 1993, 70: 3611
6. I. M. Mikhailovskij, E. V. Sadanov, T. I. Mazilova, V. A. Ksenofontov, and O. A. Velicodnaja, Phys. Rev. B, 2009, 80: 165404
7. T. T. Tsong and E. W. Müller, Phys. Rev., 1969, 181: 530
8. T. T Tsong and E. W. Müller, Phys. Rev. Lett., 1970, 25:

911
9. D. B. Joag, P. L. Kanitkar, M. M. Kanitkar, and V. M. Shukla, Bull. Mater. Sci., 1984, 6: 573
10. E. Ganz, S. K. Theiss, I. S. Hwang, and J. Golovchenko, Phys. Revs. Lett., 1992, 68: 1567
11. B. S. Swartzentruber, Phys. Rev. Lett., 1996, 76: 459
12. K. D. Wang, C. Zhang, M. M. T. Loy, and X. D. Xiao, Phys. Rev. Lett., 2005, 94: 036103
13. B. C. Stipe, M. A. Rezaei, and W. Ho, Phys. Rev. Lett., 1998, 81: 1263
14. G. Dujardin, R. E.Walkup, and P. Avouris, Science, 1992, 255: 1232
15. R. Martel, P. Avouris, and I. W. Lyo, Science,1996, 272: 385
16. T. C. Shen, C. Wang, G. C. Abeln, J. R. Tucker, J. W. Lyding, P. Avouris, and R. E. Walkup, Science, 1995, 268: 1590
17. K. Stokbro, C. Thirstrup, M. Sakurai, U. Quaade, B. Y. K. Hu, F. Perez-Murano, and F. Grey, Phys. Rev. Lett., 1998, 80: 2618
18. D. Riedel, M. L. Bocquet, H. Lesnard, M. Lastapis, N. Lorente, P. Sonnet, and G. Dujardin, J. Am. Chem. Soc., 2009, 131: 7344
19. A. D. Zhao, Q. X. Li, L. Chen, H. J. Xiang, W. H. Wang, S. Pan, B. Wang, X. D. Xiao, J. L. Yang, J. G. Hou, and Q. S. Zhu, Science, 2005, 309: 1542
20. R. Gomer, Rep. Prog. Phys., 1990, 53: 917
21. E. G. Seebauer and C. E. Allen, Prog. Surf. Sci., 1995, 49: 265
22. T. T. Tsong, Prog. Surf. Sci., 2000, 64: 199
23. J. V. Barth, Surf. Sci. Rep., 2000, 40: 75
24. T. Ala-Nissila, R. Ferrando, and S. C. Ying, Adv. Phys., 2002, 51: 949
25. S. Arrhenius, Zeit. Phys. Chem., 1889, 4: 226
26. A. Fick, Ann. Phys., 1855, 170: 59
27. L. S. Darken, Trans. Am. Inst. Mineral. Met. Eng., 1948, 175: 184
28. R. Lewis and R. Gomer, Nuovo Cimento, 1967, Suppl. I 5: 506
29. R. Gomer, Appl. Phys. A, 1986, 39: 1
30. J. E. Reutt-Robey, D. J. Doven, Y. J. Chabal, and S. B. Christman, Phys. Rev. Lett., 1988, 61: 2778
31. J. E. Reutt-Robey, D. J. Doven, Y. J. Chabal, and S. B. Christman, J. Chem. Phys., 1990, 93: 9113
32. V. J. Kwasniewski and L. D. Schmidt, Surf. Sci., 1992, 274: 329
33. H. Froitzheim and M. Schulze, Surf. Sci., 1994, 320: 85
34. X. D. Zhu, Th. Rasing, and Y. R. Shen, Phys. Rev. Lett., 1988, 61: 2883
35. J. W. Ma, X. D. Xiao, N. J. DiNardo, and M. M. T. Loy, Phys. Rev. B, 1998, 58: 4977
36. J. W. Ma, X. D. Xiao, and M. M. T. Loy, Surf. Sci., 1999, 436: L661
37. J. W. Ma, L. Cai, X. D. Xiao, and M. M. T. Loy, Surf. Sci., 1999, 425: 131
38. X. R. Wang, X. Xiao, and Z. Zhang, Surf. Sci., 2002, 512: L361
39. G. Binnig, H. Fuchs, and E. Stoll, Surf. Sci., 1986, 169: L295
40. M. L. Lozano and M. C. Tringides, Europhys. Lett., 1995, 30: 537
41. S. Renisch, R. Schuster, J. Wintterlin, and G. Ertl, Phys. Rev. Lett., 1999, 82: 3839
42. S. Horch, H. T. Lorensen, S. Helveg, E. Laegsgaard, I. Stensgaard, K. W. Jacobsen, J. K. Nørskov, and F. Besenbacher, Nature (London), 1999, 398: 134
43. R. Schaub, E. Wahlstrom, A. Ronnau, E. Laegsgaard, I. Stensgaard, and F. Besenbacher, Science, 2003, 299: 377
44. E. Wahlstrom, E. K. Vestergaard, R. Schaub, A. Ronnau, M. Vestergaard, E. Laegsgaard, I. Stensgaard, and F. Besenbacher, Science, 2004, 303: 511
45. R. M. Trump, R. J. Hamers, and J. E. Demuth, Phys. Rev. B, 1986, 34: 1388
46. P. Sobotík, P. Kocán, and I. Ošt'ádal, Surf. Sci., 2003, 537: L442
47. K. D. Wang, G. Chen, C. Zhang, M. M. T. Loy, and X. D. Xiao, Phys. Rev. Lett., 2008, 101: 266107
48. C. Zhang, G. Chen, K. D. Wang, H. W. Yang, T. Su, C. T. Chan, M. M. T. Loy, and X. D. Xiao, Phys. Rev. Lett., 2005, 94**:** 176104
49. G. Chen, X. D. Xiao, Y. Kawazoe, X. G. Gong, and C. T. Chan, Phys. Rev. B, 2009, 79: 115301
50. K. Takayanagi, Y. Tanishiro, M. Takahashi, and S. Takahashi, Surf. Sci., 1985, 164: 367
51. J. L. Li, J. F. Jia, X. J. Liang, X. Liu, J. Z. Wang, Q. K. Xue, Z. Q. Li, J. S. Tse, Z. Zhang, and S. B. Zhang, Phys. Rev. Lett., 2002, 88: 066101
52. O. Custance, S. Brochard, I. Brihuega, E. Artacho, J. M. Soler, A. M. Baró and J. M. Gómez-Rodríguez, Phys. Rev. B, 2003, 67: 235410
53. K. Wu, Y. Fujikawa, T. Nagao, Y. Hasegawa, K. S. Nakayama, Q. K. Xue, E. G. Wang, T. Briere, V. Kumar, Y. Kawazoe, S. B. Zhang, and T. Sakurai, Phys. Rev. Lett., 2003, 91: 126101
54. C. M. Chang and C. M. Wei, Phys. Rev. B, 2003, 67: 033309
55. P. Hohenberg and W. Kohn, Phys. Rev. B, 1964, 136: 864
56. W. Kohn and L. J. Sham, Phys. Rev. A, 1965, 140: 1133
57. K. Cho and E. Kaxiras, Europhys. Lett., 1997, 39: 287
58. K. Cho and E. Kaxiras, Surf. Sci., 1998, 396: L261
59. K. D. Wang, F. F. Ming, Q. Huang, X. Q. Zhang, and X. D. Xiao, Surf. Sci., 2010, 604: 322
60. M. A. Henderson, A. Szabo, and J. T. Yates Jr., J. Chem. Phys., 1989, 91: 7245
61. M. A. Henderson, A. Szabo, and J. T. Yates Jr., J. Chem. Phys., 1989, 91: 7255
62. H. R. Siddiqui, X. Guo, I. Chorkendorff, and J. T. Yates Jr., Surf. Sci., 1987, 191: L813
63. D. M. Collins and W. E. Spicer, Surf. Sci., 1977, 69: 85
64. J. S. Luo, R. G. Tobin, D. K. Lambert, G. B. Fisher, and

C. L. Dimaggio, Surf. Sci., 1992, 274: 53
65. X. F. Cui, B. Wang, Z. Wang, T. Huang, Y. Zhao, J. L. Yang, and J. G. Hou, J. Chem. Phys., 2008, 129: 044703
66. L. Gao, Q. Liu, Y. Y. Zhang, N. Jiang, H.G. Zhang, Z. H. Cheng, W. F. Qiu, S. X. Du, Y. Q. Liu, W. A. Hofer, and H. J. Gao, Phys. Rev. Lett., 2008, 101: 197209
67. Q. Liu, Y. Y. Zhang, N. Jiang, H. G. Zhang, L. Gao, S. X. Du, and H. J. Gao, Phys. Rev. Lett., 2010, 104: 166101
68. R. L. Carroll and C. B. Gorman, Angew. Chem. Int. Ed., 2002, 41: 4378
69. J. A. Stroscio, F. Tavazza, J. N. Crain, R. J. Celotta, and A. M. Chaka, Science, 2006, 313: 948
70. Y. F. Wang, X. Ge, G. Schull, R. Berndt, H. Tang, C. Bornholdt, F. Koehler, and Ra. Herges, J. Am. Chem. Soc., 2010, 132: 1196
71. Y. F. Wang, J. Kroger, R. Berndt, and W. A. Hofer, J. Am. Chem. Soc., 2009, 131: 3639
72. Y. F. Wang, X. Ge, G. Schull, R. Berndt, C. Bornholdt, F. Koehler, and R. J. Herges, J. Am. Chem. Soc., 2008, 130: 4218
73. T. Komeda, Y. Kim, Y. Fujita, Y. Sainoo, and M. Kawai, J. Chem. Phys., 2004, 120: 15